Journal of Neurochemistry
Lippincott-Raven Publishers, Philadelphia

Enhanced Hemicholinium Binding and Attenuated Dendrite Branching in Cognitively Impaired Acetylcholinesterase-Transgenic Mice

R. Beeri, *N. Le Novère, †R. Mervis, T. Huberman, ‡E. Grauer, *J. P. Changeux, and H. Soreq

*Department of Biological Chemistry, Life Sciences Institute, Hebrew University of Jerusalem, Jerusalem; ‡Department of Pharmacology, Israel Institute for Biological Research, Ness-Ziona, Israel; *Molecular Neurobiology Laboratory, Biotechnologies Department, Pasteur Institute, Paris, France; and †Neuro-Cognitive Research Laboratories, Columbus, Ohio, U.S.A.*

Abstract: In a search for behavioral, neuroanatomical, and metabolic characteristics of Alzheimer's disease that may result from cholinergic malfunction, we used transgenic mice overexpressing acetylcholinesterase (AChE) mRNA and active enzyme in brain neurons. Mapping by in situ hybridization revealed that transgenic and host AChE mRNAs were distributed similarly. In a Morris water maze working memory paradigm, adult transgenic mice did not display the characteristic improvement found in control mice either between or within test days and spent less time than control mice in the platform zone. In 5-week-old transgenic mice, the basilar dendritic trees of layer 5 pyramidal neurons from the frontoparietal cortex were essentially as developed as in age-matched controls. However, branching totally ceased after this age, whereas in control adults it continued up to at least 7 months. Therefore, dendritic arbors became smaller in adult transgenic mice than those of controls. Furthermore, the average number of spines was significantly lower on dendritic branches of 7-month-old but not 5-week-old transgenics as compared with controls. Binding of tritiated hemicholinium-3, a blocker of the high-affinity choline uptake characteristic of active cholinergic terminals, was over twofold enhanced in the brain of transgenic mice. In contrast, no differences were observed in the mRNA and ligand binding levels of several different subtypes of nicotinic and muscarinic acetylcholine receptors. These findings suggest that three different hallmarks associated with Alzheimer's disease—namely, progressive cognitive failure, cessation of dendrite branching and spine formation, and enhanced high-affinity choline uptake—are outcomes of cholinergic malfunction. **Key Words:** Acetylcholinesterase—Alzheimer's disease—Choline uptake—Dendritic fields—Spines—Memory deficit.
J. Neurochem. **69,** 2441–2451 (1997).

Animal models for studying late-onset disorders associated with cholinergic deterioration and most notably Alzheimer's disease (AD) should display progressive deterioration of memory and learning, as well as senile plaques and neurofibrillary tangles (Price et al., 1995), a hypofunctional cholinergic system (Bierer et al., 1995), and breakdown in cortical circuitry related to cell and synaptic loss (Davies and Maloney, 1976; DeKosky and Scheff, 1990; Honer et al., 1992; Terry et al., 1992). Aged, cognitively impaired animal models displayed the expected behavioral, neuroanatomical, and/or neurochemical changes in their cholinergic system (Bartus and Uemura, 1979). Several physical or pharmacological modulations also resulted in loss of cholinergic synapses and impaired memory (Fischer et al., 1989; Zhi et al., 1995). Subsequently transgenic amyloid precursor protein mouse models (Games et al., 1995; Hsiao et al., 1995, 1996; LaFerla et al., 1995; Moran et al., 1995) demonstrated development of amyloid β protein deposits, neuritic plaques, synaptic loss, and late-onset spatial memory deficits. However, in AD, amyloid plaques and tangles are particularly concentrated in brain regions where cholinergic circuits operate (Coyle et al., 1983). Also, synaptic loss but not the presence of amyloid plaques or neurofibrillary tangles could be convincingly correlated with cognitive impairment in AD (Terry et al., 1992). Yet, correlation between high levels of β-amyloid deposits and progressive severity of the cognitive defect was only shown in some of the above transgenic models (Hsiao et al., 1996). Therefore, it remained unresolved

Received April 23, 1997; revised manuscript received June 19, 1997; accepted July 9, 1997.

Address correspondence and reprint requests to Dr. H. Soreq at Department of Biological Chemistry, Life Sciences Institute, Hebrew University of Jerusalem, Jerusalem 91904, Israel.

Abbreviations used: ACh, acetylcholine; AChE, acetylcholinesterase; AChR, acetylcholine receptor; AD, Alzheimer's disease; ChAT, choline acetyltransferase; MGV, mean gray value; OD, optical density; RT-PCR, reverse transcription-polymerase chain reaction.

whether the learning deficits in these mice were caused by or only correlated with increased brain amyloid β peptide levels and amyloid depositions.

In AD, structural changes in brain cholinergic synapses (DeKosky and Scheff, 1990) are associated with loss of neuronal nicotinic binding sites (Nordberg et al., 1988), with death of acetylcholine (ACh)-producing neurons (Davies and Maloney, 1976; Whitehouse et al., 1986), and with the consequent disruption of cholinergic neurotransmission (Coyle et al., 1983; Fibiger, 1991). The resultant hypocholinergic condition is characterized by a relative excess of the ACh-hydrolyzing enzyme acetylcholinesterase (AChE). To define the contribution of cholinergic malfunction toward the AD phenotype, we have recently used the authentic promoter from the human ACHE gene in conjunction with the AChE-coding sequence to create transgenic mice expressing human AChE in CNS neurons. Manual use of the Morris water maze revealed a progressively severe decline in the spatial learning and memory capabilities of these transgenic mice (Beeri et al., 1995). It was therefore of interest to dissect carefully the learning and memory impairments in AChE-transgenic mice and examine in them which of the morphometric and/or biochemical correlates of AD can be causally associated with cholinergic malfunction.

Cortical neurons in normal aged humans may develop longer and more branched dendritic trees than those in either young adults or individuals with senile dementia (Buell and Coleman, 1981). Cognitive deficiencies are further associated with dysgenesis of dendritic spines, on which most cortical synapses reside (Purpura, 1974; Braak and Braak, 1985). We therefore wished to evaluate the state of dendrite arborizations and spine density in adult transgenic mice with excess brain AChE. Also, we explored the transport of choline, which is used by cholinergic neurons, both for reforming metabolized membrane phosphatidylcholine and for synthesizing the neurotransmitter ACh. The levels of the high-affinity Na^+-dependent choline transporter unique to these cells can be quantified using [^{3}H]hemicholinium-3 (Vickroy et al., 1984). The concentration of available choline is the rate-limiting factor for ACh synthesis: When choline is in short supply, active cholinergic neurons were reported to sustain neurotransmission at the expense of membrane building (Wurtman, 1992). Indeed, cerebral cortical areas in AD brains exhibited marked decreases in choline acetyltransferase (ChAT) activity and significant enhancement in [^{3}H]hemicholinium-3 binding. In the AD frontal cortex, transporter overexpression exceeded the level that is needed to compensate for the loss of synaptic terminals, presumably accelerating membrane turnover and neurodegeneration (Slotkin et al., 1994).

In the search for behavioral, morphological, and molecular correlates common to AD and the AChE-transgenic mice we used video imaging to assess carefully the memory impairment in these mice. We further examined in them the dendritic branching and spine density in cortical neurons, the mRNA and protein levels of ACh receptors (AChRs), and the levels of [^{3}H]hemicholinium-3 binding. Our findings demonstrate complex cognitive failure, attenuated dendrite branching, decreased spine density, and imbalanced choline metabolism in AChE-transgenic mice, with all of these phenomena being attributed to AChE excess and the associated cholinergic malfunction.

MATERIALS AND METHODS

Mice

FVB/N mice carrying human AChE cDNA under the control of 586 bp of the authentic human AChE promoter were constructed and identified as described (Beeri et al., 1995; Andres et al., 1997). Age- and sex-matched wild-type FVB/N mice served as controls.

In situ hybridizations

For radioactive in situ hybridization, cryostat-cut brain sections were hybridized with 45-mer oligodeoxynucleotides end-labeled with [α-^{33}P]dATP (Boehringer-Mannheim, Germany), according to the manufacturer's recommendations. Prehybridization, hybridization, and washings were as described elsewhere (Le Novère et al., 1996). The probes used were targeted toward rat nicotinic AChR subunits α3, 4, 5, and 7 and β2, 3, and 4. Discriminative probes of AChE were as follows: human ACHE, 5′-GACACCAGCACAGTCCTGTCGGCCTGTACCAAGAAGCGGCCATCG-3′; mouse ACHE, 5′-GATACCAACACAGCTCCCTCAACCTGGGCCAGGAAACGGCCGTCA-3′. Genbank accession numbers for the sequences targeted by these probes are L31621, M15681, J05231, M85273, L31622, J04636, J05232, M55040, and X56518, respectively. These sequences can be electronically retrieved at Le Novère and Changeux (1995).

High-resolution nonradioactive in situ hybridization with 2-*O*-methyl biotinylated mouse AChE cRNA (exon 6), streptavidin–alkaline phosphatase conjugate, and fast red substrate was performed on 5-μm-thick paraffin brain sections as detailed elsewhere (Andres et al., 1997). Three sections from different brain levels of three individual mice (control and transgenic) were used.

Morris water maze test

Mice were tested in a circular black pool, 140 cm in diameter and 50 cm high, filled to the height of 24 cm with water (at ~23°C). The pool was divided by imaginary lines into four quadrants of equal size and three concentric zones. A black painted platform was placed in the center of a quadrant (in the middle zone) of the pool with its top surface (12 × 12 cm) located <1 cm below water level. The pool was placed in the center of a well-lit room with ample cues that were kept constant throughout the testing period. The performance of the mice was monitored by a video tracking system (HVS IMAGE; Ormond Crescent, Hampton, U.K.), thus enabling detailed analysis of the swimming pattern.

Path length, latency to reach the platform, and swimming speed were simultaneously recorded, as well as the percentage of time spent in each quadrant and zone. Mice were tested in two successive trials (2 h apart) per day. Each trial began by placing the mouse on the platform for 30 s, after

(Fig. 2B); however, in buffers containing sodium bromide, sodium formate, or sodium iodide, significant levels of taurine transport activity (77, 41, and 15%, respectively) are observed (Fig. 2B). Because replacement of Cl^- with gluconate virtually abolished the taurine uptake (Fig. 2B), we do not think that the taurine uptake levels in the sodium bromide, sodium formate, and sodium iodide buffers are by any means influenced by the gluconate salts of calcium, magnesium, and potassium that are present in these buffers (see Materials and Methods for buffer compositions). The above data clearly demonstrate that the taurine transport via the taurine transporter requires both Na^+ and Cl^- under physiological conditions; furthermore, the transporter has a higher selectivity for Na^+ than for Cl^-.

Biochemical properties

Taurine transport assays conducted with various extracellular concentrations of [^{3}H]taurine indicate that the rate of taurine uptake increases hyperbolically when the external concentration of taurine is increased (data not shown). This saturation process follows Michaelis–Menten kinetics, because analysis of the data by Eadie–Hofstee plot is linear (data not shown). The apparent K_m for taurine, determined from the Eadie–Hofstee plots of two independent experiments, is 11.5 and 14.8 μM, respectively. This observed K_m value for taurine is within the same range as those reported for the mouse brain (K_m = 4.5 μM; Liu et al., 1992), human placental (K_m = 5.9 μM; Ramamoorthy et al., 1994*a*), and rat brain (K_m = 40 μM; Smith et al., 1992) taurine transporters. In preliminary studies, we have obtained an apparent K_m of ~15 μM for taurine by electrophysiological technique using mTAUT (Loo et al., 1996).

Because the taurine transport activity induced by mTAUT in *Xenopus* oocytes depends on both Na^+ and Cl^-, we examined how the rate of taurine uptake changes when the external concentration of both Na^+ and Cl^- was varied independently. When the external concentration of Cl^- was varied, the rate of taurine uptake increased hyperbolically (Fig. 3B). In contrast, when the external concentration of Na^+ was varied, the rate of taurine uptake showed a sigmoidal dependence (Fig. 3A).

Because the rate of taurine uptake varies hyperbolically with the external Cl^- concentration and follows Michaelis–Menten-type single saturation kinetics, it suggests that one Cl^- is required for the transport of taurine via the transporter. Eadie–Hofstee transformation of the data shows linearity and supports the above notion (Fig. 3B, inset). As determined from three independent experiments, the rate of taurine uptake saturated with an average equilibrium constant, K_{Cl^-}, of 17.7 mM when the external Cl^- concentration was varied. The sigmoidal relationship seen when the external concentration of Na^+ was varied suggests that more than one Na^+ is required for the transport of taurine by the transporter. To calculate the number of Na^+ involved, experimental data were analyzed by nonlinear regression curve fit analysis and by the Hill plot (Fig. 3A). From the curve fit analysis, the rate of taurine uptake saturated with an equilibrium constant, K_{Na^+}, ~54.8 mM when the external Na^+ concentration was varied. The Hill coefficient (n) determined from the curve fit analysis (n = 2.18) and the slope of the linear Hill plot (n = 2.06) is close to 2, suggesting that at least two Na^+ are required for the transport of each taurine molecule. In preliminary studies, similar coupling ratios (2 Na^+/1 Cl^-/1 taurine) have been observed for mTAUT using electrophysiological technique (Loo et al., 1995).

The calculated pI for the mTAUT is 6.96, a significantly lower value than the reported pI for the human taurine transporter (pI ~8.3; Ramamoorthy et al., 1994*a*). The difference in the pI values between these two highly homologous taurine transporters suggests that the two transporters may exhibit different pH-activity profiles. None of the earlier studies examined the pH dependency of the taurine transporter. To investigate the pH-activity profile of the mTAUT, we have varied the pH of the external NaCl transport buffer and examined its effect on the rate of taurine transport (Fig. 4). A minimal taurine transport activity is seen between pH 6.0 and 6.5 and a maximal activity between pH 7.5 and 8.0. Because of technical problems, we were unable to examine the effect of external pH on the rate of taurine uptake beyond the pH window of 5.3–8.5; moreover, we do not know whether the observed inhibition of taurine uptake activity at pH >8.0 is due to a toxic effect of the transport buffer on the oocytes. Nevertheless, it is clear from the above results that the activity of the mTAUT is pH dependent. To our knowledge, this is the first demonstration of the effect of pH on the activity of a transporter belonging to the Na^+- and Cl^--dependent GABA transporter superfamily.

Pharmacological properties

Assays conducted with various compounds confirm that the taurine uptake induced by mTAUT is inhibited by many known taurine transporter inhibitors. Table 1 summarizes the calculated IC_{50} value of various compounds determined from their dose–response relationship plot. Based on these analyses, the order of potency of various compounds inhibiting the taurine transport is as follows: hypotaurine > β-alanine > L-DAPA > GES > β-GPA > chloroquine > GABA > homotaurine. No inhibitory effect was observed with 1 mM glycine or DL-carnitine. It is noteworthy that GABA and β-GPA, an inhibitor of the mouse GABA transporters (Liu et al., 1993), inhibit [^{3}H]taurine transport activity in the oocytes. The latter inhibits the mTAUT activity more effectively than GABA itself. In contrast, two other known GABA transporter inhibitors, L-diaminobutyric acid and nipecotic acid, did not inhibit the taurine transport at concentrations of 1 mM and 200

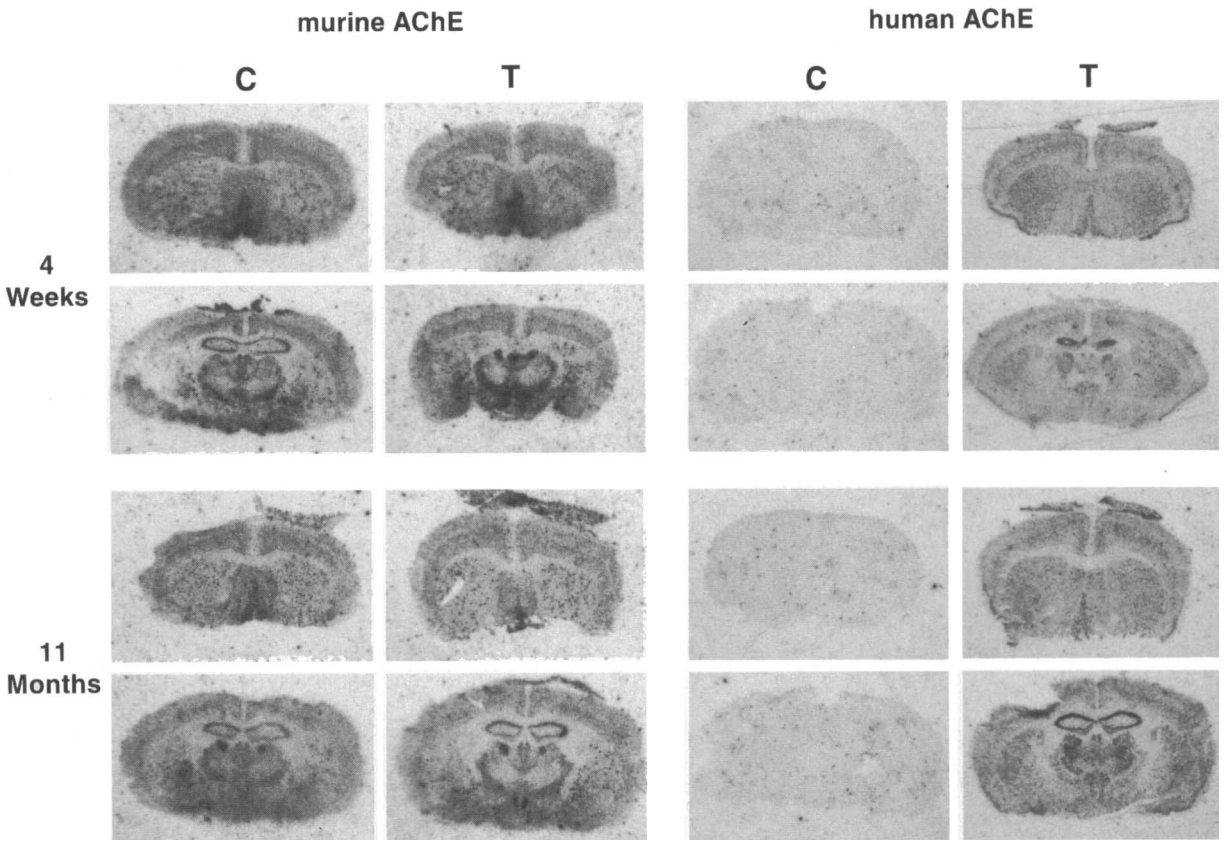

FIG. 1. Transgenic human AChE mRNA is coexpressed with host mouse AChE mRNA, shown by in situ hybridization of the murine and human AChE mRNA in control (C) and transgenic (T) mice. Note the small dots in the striatum of the sections hybridized with the probe for the endogenous AChE, which represent the striatal cholinergic interneurons.

Impaired performance in the Morris water maze

To dissect the progressive cognitive impairment that was initially identified in these mice by manual follow-up of the Morris water maze (Beeri et al., 1995), 5-month-old AChE-transgenic (n = 11) and control (n = 19) mice were compared in the Morris water maze by video imaging and dedicated software. Control mice showed a gradual decrease in the mean latency to reach the platform over days, indicating intact reference memory (Fig. 3A). In contrast, transgenic mice failed to show improvement over time (group × days effect, $F_{4,108} = 5.92$, $p < 0.001$), which suggests impaired reference memory (Fig. 3C). In addition, control mice showed a mild improvement in the overall performance of the second trial as compared with the first one within the same day (this limited improvement may result from the long delay between the two trials). Transgenic mice showed no such improvement within the daily trials (group × trials effect, $F_{1,27} = 4.14$, $p = 0.05$), suggesting an impaired working memory (Fig. 3A and C). Transgenic mice were further significantly different from control mice in their mean swimming speed (group main effect, $F_{1,27} = 17.7$, $p < 0.001$; Fig. 3B and D). Because this speed difference between the groups remained constant throughout the test period, it cannot account for the increased difference in latency performance between the two groups, which developed over time. Rather, this physical parameter probably reflects the progressive neuromotor decline displayed by these mice (Andres et al., 1997).

Control animals showed improved search strategy seen as an increase in the time spent in the concentric middle zone, where the platform was located (Fig. 3E). No such increase was seen in the group of transgenic mice (Fig. 3E; group main effect, $F_{1,27} = 20.7$, $p < 0.001$), which showed a significant tendency to remain near the pool wall, i.e., thigmotaxis (Fig. 3F; group main effect, $F_{1,27} = 9.67$, $p < 0.001$). The thigmotaxis may reflect higher sensitivity to stress. Combined effects of memory impairment and increased sensitivity to stress were also demonstrated in the cholinergically impaired WKY rat strain (Grauer and Kapon, 1993).

Attenuated dendritic branching and reduced spine numbers in midaged human promoter AChE-transgenic mice

Assessment of dendritic branching of Golgi-impregnated cortical neurons was carried out in 7-month-old and 5-week-old transgenics and age-matched controls

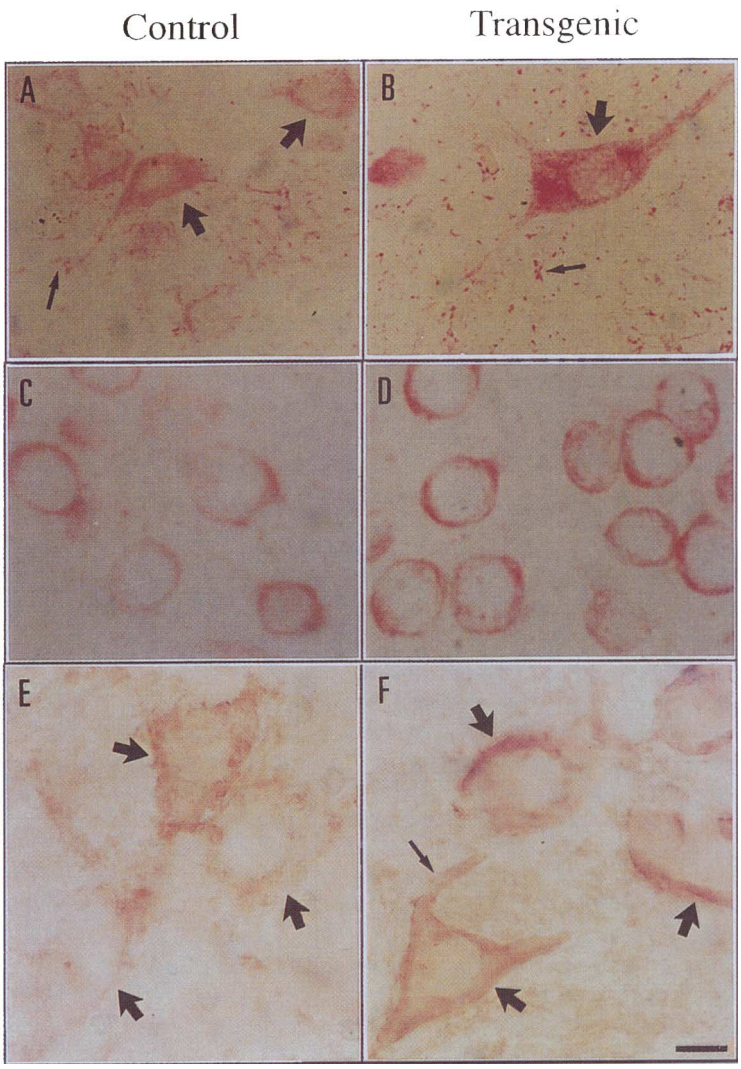

FIG. 2. AChE overexpression in neostriatal neurons. **Upper and middle panels:** AChE mRNA. Presented are paraffin-embedded neostriatum (**A** and **B**) and cortex sections (**C** and **D**) from control (A and C) and transgenic (B and D) mice following in situ hybridization with a 5′-biotinylated AChE cRNA probe detecting both mouse and human AChE mRNA. **Lower panels:** Active AChE. Presented are floating Vibratome-cut sections cytochemically stained for acetylthiocholine hydrolysis from (**E**) control and (**F**) transgenic mice. Because of the different treatments involved in these two procedures, the neurons appear somewhat shrunken in the paraffin-embedded sections. Judging by the heavier staining in neurons from transgenic mice as compared with controls, both cell bodies and apical processes of neostriatal neurons contain both the human mRNA and its human enzyme product. Sites of heavy staining are denoted in neuronal processes by thin arrowheads and in cell bodies by thick arrowheads. Bar = 10 μm.

(four animals per group). Figure 4A presents examples of such Golgi staining. Camera lucida drawings of the basilar tree of nine randomly selected layer V pyramidal cells from the frontoparietal cortex of each group (see examples in Fig. 4B) were further evaluated by Sholl analysis. The dendritic arbors in 7-month-old control brains were slightly larger than those of 5-week-old controls ($p \leq 0.6$), whereas dendritic arbors of transgenic neocortical pyramidal neurons were smaller in 7-month-old animals ($p \leq 0.060$) than in 5-week-old ones. The combined effects of the upward age-related small shift in the controls and greater downward shift in the transgenics resulted in significant differences between dendritic domains of neurons from the 7-month-old transgenic and control mice ($n = 36$; $p \leq 0.011$ using a Gaussian approximation; Fig. 4C and Table 1). AChE overexpression therefore had a detrimental effect on maintenance of the dendritic arbor. The onset of this effect coincided with the onset of the progressive cognitive failure in these transgenic mice (Beeri et al., 1995), suggesting a causal relationship between these two AD-characteristic phenomena (Buell and Coleman, 1981; Katzman, 1986).

Dendritic spines of the basilar tree, which represent the loci for the vast majority of all synaptic input to the neuron, were counted along the entire dendritic branch (from the terminal tips to first-order branches) of three to five branches per randomly selected seven neurons per brain. As seen in Table 1, in comparison with age-matched controls the 5-week-old transgenic mice showed no significant differences in the average number of spines per basilar tree. In contrast, neurons from the 7-month-old cognitively impaired transgenic mice had significantly fewer spines ($p \leq 0.040$) in comparison with those from 7-month-old controls (Table 1). By 7 months, the number of spines in control mice increased by 10% from that of 5 weeks, whereas in transgenics it decreased by 15% (Table 1). This led to a highly significant difference in the total number of dendritic spines per cell ($p \leq 0.0055$ by unpaired

t test). Figure 4D presents examples for the reduced spine number in adult but not young transgenic neurons.

No apparent adjustment in cholinergic receptors

Reduction in levels of nicotinic AChRs has been reported in AD (Whitehouse et al., 1986; Nordberg et al., 1988; Perry et al., 1995). Therefore, we examined in AChE-transgenic mice the protein and mRNA levels of several AChR subtypes. Also, we considered other potential levels for up-regulating receptor binding capacities, e.g., translation efficiency, protein stability, and allosteric modulation of binding properties (Heidmann and Changeux, 1978). To this end, the binding levels of different nicotinic and muscarinic agonists were examined in frozen coronary brain sections from transgenic and control mice.

Levels of mRNA for neuronal nicotinic AChR $\alpha 3-5$, $\alpha 7$, and $\beta 2-4$ subunits were examined by in situ hybridization to coronary brain sections from several brain regions of 4-week-, 5-month-, and 11-month-old transgenic and control mice. Hybridization signals revealed no apparent difference in signal localization and intensity between control and transgenic mice of all ages (Fig. 5 and data not shown). In addition, semiquantitative RT-PCR analyses revealed similar levels of the mRNAs for nicotinic AChR $\alpha 4$ and M1 muscarinic AChR mRNAs in control and transgenic brains (data not shown). Binding levels of [*N-methyl*-[^{3}H]pirenzepine and [2,3-*dipropylamino*-^{3}H]AF-DX 384 reflected M1 and M2 muscarinic AChRs, respectively. Binding of ^{125}I-α-bungarotoxin revealed the $\alpha 7$-containing nicotinic AChR, and [^{3}H]nicotine, [^{3}H]-cytisine, and [^{3}H]epibatidine detected $\alpha 2-6$, $\beta 2-4$-containing nicotinic AChRs. All remained unchanged in both young and old transgenic mouse brains as compared with controls (Fig. 5 and data not shown).

Although the methods we used to assess receptor production and binding capacities would probably overlook minor modifications, these analyses gave clear indication for the lack of major changes in the transcription and/or stability of the mRNA for several nicotinic AChRs and muscarinic AChR subunits as well as in their corresponding protein products. That most of the nicotinic AChR and muscarinic AChR subunits were present in the AChE-transgenic brain in normal levels and binding capacities and the presence of unmodified levels of neuronal nicotinic receptor subunits in $\beta 2$ nicotinic AChR knockout mice (Picciotto et al., 1995) therefore supports the notion that the transcriptional and/or posttranscriptional control of AChR production is not associated with cholinergic imbalance processes in the mammalian brain.

Enhanced levels of high-affinity choline transporter in transgenic mouse brain

We examined whether changes occurred in choline uptake by incubating coronal brain sections with [^{3}H]-hemicholinium-3, the effective blocker of the high-affinity Na^+-dependent choline transporter (Vickroy et al., 1984). The autoradiographic distribution of [^{3}H]hemicholinium-3 binding sites correlated with the distribution of classical presynaptic markers of the cholinergic system and was associated with the presence of cholinergic terminals. High-density binding sites were found in striatum, amygdala, and interpeduncular nucleus, and labeling density was much lower in the cortex and hippocampus (Forloni and Angeretti, 1992; data not shown). Twofold higher levels of hemicholinium binding were found in the neostriatum of young (4-week-old) and midaged (11-month-old) transgenics as compared with control mice (Fig. 6). It is interesting that the enhancement of hemicholinium binding to frontal cortex sections from Alzheimer's brains was also twofold (Slotkin et al., 1994). Similar enhancement in hemicholinium binding was also found in the cholinoceptive interpeduncular nucleus of transgenic mice but not in their hippocampus (data not shown). In contrast, semiquantitative RT-PCR revealed no difference in the mRNA levels between control and transgenic brain for the ACh-synthesizing enzyme ChAT, the vesicular protein synaptophysin that serves as general synaptic marker (Leube et al., 1987), and L-type Ca^{2+} channel α subunit (data not shown). This was so at both the ages of 4–5 weeks and 11–12 months, which excludes the possibility of late-onset changes. Therefore, hemicholinium binding was selectively enhanced in both cholinergic and cholinoceptive brain regions of AChE-overexpressing mice, where a high density of binding sites was reported in normal brain (Forloni and Angeretti, 1992).

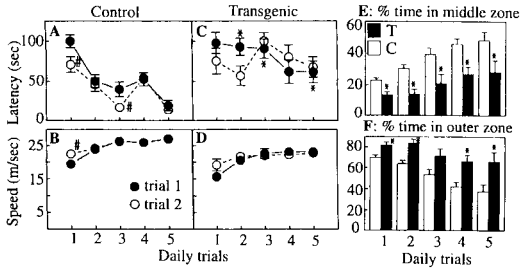

FIG. 3. Impaired performance of adult transgenic mice in a working memory procedure in the water maze. Improved mean ± SEM (bars) latency to reach the platform in trial 1 in control (n = 19; **A**) as compared with transgenic (n = 11; **C**) mice indicates changes in reference memory. Improved performance in trial 2 versus trial 1 indicates changes in working memory. **B** and **D**: Somewhat lower swimming speed occurs in transgenic as compared with control mice. **E** and **F**: Percent time spent in middle and outer concentric zones suggests an impaired search strategy of transgenic mice. $^*p < 0.05$ for transgenic versus control; $^\#p < 0.05$ trial 1 versus trial 2. See text for detailed statistical analysis.

DISCUSSION

Transgenic mice overexpressing AChE in their brain neurons suffer complex impairments in learning and memory, late-onset attenuation of dendrite branching

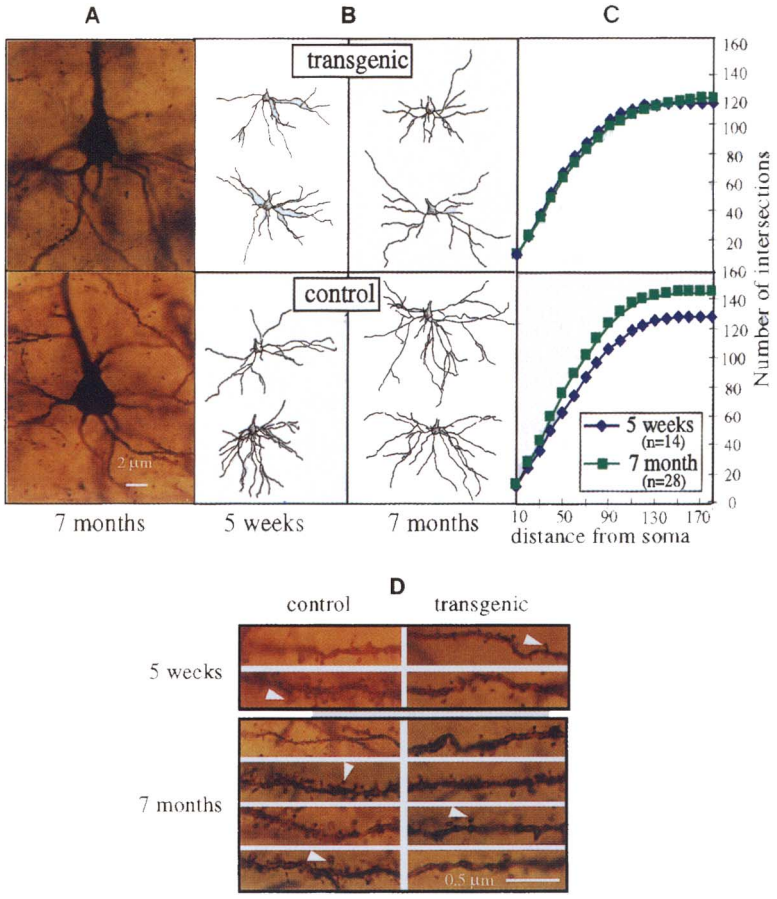

FIG. 4. Attenuated dendritic branching and spine loss in layer 5 pyramidal neurons from the frontoparietal cortex of transgenic mice. **A:** Representative Golgi-stained preparations from brains of transgenic (**top panel**) and control (**bottom panel**) 7-month-old mice. **B:** Camera lucida tracings of the basilar tree of Golgi-stained pyramidal neurons from the frontoparietal cortex of 5-week- and 7-month-old transgenic and control brains. **C:** Graphical presentations of data from Sholl analyses. Shown are numbers of dendritic branches intersecting with a series of concentric circles of increasing distance from the cell body. Numbers of intersections are expressed as a cumulative total. See text and Table 1 for details. **D:** Representative high-magnification photographs of dendritic branches from 5-week- and 7-month-old transgenic and control mice. Note the reduction in spines (arrowheads) on the transgenic dendrites.

in pyramidal neurons within the frontoparietal cortex, and enhanced binding capacity of the high-affinity Na^+-dependent choline transporter in the neostriatum. Young mice, at the age of 4–5 weeks, exhibit less severe depletions than older adult animals, at the age of 7–11 months, representing a progressive, complex cognitive decline which these mice undergo. This supports the notion that these phenotypic sequelae are related to the cholinergic deficit also in AD patients.

Complex memory impairments

The impairment in both working and reference memory in AChE-transgenic mice is more severe and complex compared with other models with cholinergic deficits. Apolipoprotein E-deficient mice, which revealed reduced ChAT activities and impaired hypothermic responses to the cholinergic agonist oxotremorine, suffered impairments in working but not reference memory (Gordon et al., 1995). Working but not reference memory is selectively vulnerable to central cholinergic blockade as well as to medial septal and hippocampal lesions (Gordon et al., 1995). One recent model in which reference memory was impaired was based on overexpression of the mutant 695-amino-acid isoform of β-amyloid precursor protein (Hsiao et al., 1996). However, the performance of mutant β-amyloid-expressing mice improved in the Morris water maze even at the age of 10 months, unlike our mice, which totally failed to improve performance at as early as 5 months of age. The authentic overexpression of AChE in cholinergic neurons (Beeri et al., 1995; Andres et al., 1997; present study) may explain the severity of these cognitive phenotypes. Also, AChE-transgenic mice revealed a significant tendency to thigmotaxis, similar to rats administered scopolamine (Hodges, 1996). As habituation to stress improved water maze performance of old rats, which tend to exhibit thigmotaxis (Mabry et al., 1996), our results may indicate that AChE overexpression and/or the resultant cholinergic imbalance creates higher sensitivity to stress conditions.

Attenuated dendritic branching and loss of spines in cortical neurons

Loss of synapses and neurons has repeatedly been demonstrated to correlate with the degree of cognitive impairment in AD (DeKosky and Scheff, 1990). In the adult nervous system, continuous changes in the size and shape of the dendritic tree involve dendritic retraction and elongation, formation of new branches,

TABLE 1. *Progressive deterioration of layer V pyramidal neurons in AChE-transgenic mice*

Tested parameters	5-week-old mice		7-month-old mice		Significance of C, T comparison	
	C	T	C	T	5 weeks	7 months
1. No. of Golgi-stained neurons evaluated for dendrite branching (animal) [total]	9/(2) [18]	9/(2) [18]	9/(4) [36]	9/(4) [36]		
2. Cumulative total intersections/ neuron (Sholl analysis, at 150 μm from soma)	123	118	126	109	$p \leq 0.2323^a$	$p \leq 0.0113^a$
3. Effectiveness of C, T pairing	0.9938		0.9969		$p \leq 0.0001^b$	$p \leq 0.0001^b$
4. No. of stained neurons analyzed for dendritic spines/(animal) [total]	7/(2) [14]	7/(2) [14]	9/(4) [36]	9/(4) [36]		
5. Average no. of spines/basilar branch/neuron (mean ± SEM)	105.7 ± 9.63	99.95 ± 7.76	108.6 ± 6.49	89.91 ± 6.09	$p = 0.8378^c$	$p = 0.0398^c$
6. Difference between C, T means	5.71 ± 12.37		18.65 ± 8.90		$p = 0.2238^d$	$p = 0.03552^d$
7. Variance comparison (Mann–Whitney U value)	87.50		444.0		$p = 0.6459^e$	$p = 0.0220^e$

For parameters 1–3, using coded slides, the basilar tree of the noted no. of Golgi-stained neurons per brain in two or four animals per group (parentheses) was evaluated for branching, using Sholl analysis (method of concentric circles). Statistical analyses (specified under "significance") showed significant differences between the 7-month-old but not 5-week-old control (C) and transgenic (T) mice under highly significant pairing effectiveness. For parameters 4–7, dendritic spines were counted along the entire dendritic branch of three to five branches per randomly selected nine neurons for each brain. Both total and the average no. of spines were significantly different between 7-month-old but not 5-week-old T and C mice.

[a]Gaussian approximation of Wilcoxon test.
[b]Spearman approximation.
[c]Unpaired t test.
[d]F test of variance.
[e]Mann–Whitney test, two-tailed p value.

and creation of new synapses between them. Moreover, dendritic arborization is enhanced in the normal adult brain, under conditions of increased functional requirements (Buell and Coleman, 1981). Basilar dendritic arbors of frontal cortical neurons in aged rats are significantly larger than those of young adult rats (Wellman and Sengelaub, 1995), which is likely a compensatory response to the death of other cortical neurons (Coleman and Flood, 1987). All of these changes in dendritic arbors were apparently stopped in the brain of adult AChE-transgenic mice, accompanied by loss of dendritic spines.

Dendritic organization is primarily determined by extrinsic factors mediated through communication between dendrites of neighboring cells, the activity of afferent neuronal connections or chemotrophic factors, and intrinsic neuronal properties affecting the response to all these stimuli (Arendt et al., 1995). Lesions of the nucleus basalis magnocellularis do not significantly affect dendritic morphology in young adult rats, but cortical neurons in middle-aged and aged rats showed a marked reduction in dendritic arbors following such lesions (Wellman and Sengelaub, 1995). Quantitative studies also revealed shorter and less branched dendrites in neurons from some cortical regions of humans with senile dementia compared with normal aged individuals (Buell and Coleman, 1981). Newly formed dendrites have also been reported, but only in neurons that exhibited reduced appearance of dendritic arbors on the remaining dendrites (Ferrer et al., 1990). Dendritic growth and neuronal and spine loss can hence be regarded as bidirectional processes that occur simultaneously but result in opposite effects on the total of the dendritic network as an attempt of repair following neuronal and synapse deterioration or as primary pathological events leading to neuronal degeneration.

The late-onset attenuation of dendritic material in AChE-transgenic mice would logically represent the anatomical correlate of the progressive age-related behavioral impairments. The concomitant loss of dendritic spines may suggest that the transgenic mice at midage have impaired compensation capabilities of dendritic trees and synapses under conditions of cholinergic imbalance. The cognitive decline under dysfunction of the cholinergic system in normal elderly individuals has also been associated with age-related dendritic attenuation (McEntee and Crook, 1992; Gallagher and Colombo, 1995). In light of the rapidly increasing percentage of elderly in the population, treatment of such "normal" age-associated memory impairments should be considered as a cost-effective public health measure to delay more serious degeneration. The AChE-transgenic model may thus prove to be of particular value toward the development of therapeutic pharmaceutical strategies to attenuate (halt or

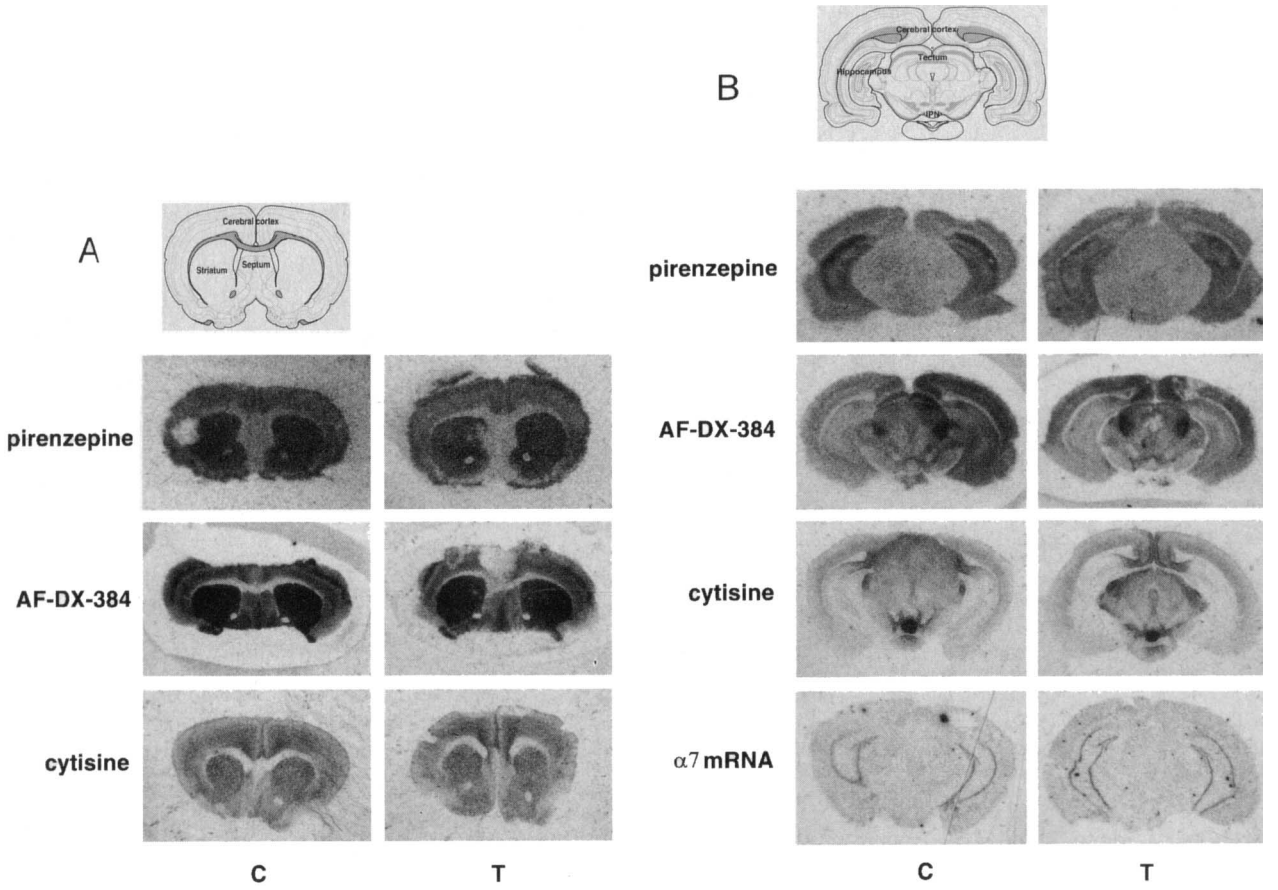

FIG. 5. Similar binding capacities to AChR subtypes in transgenic neostriatum. **A:** [^{3}H]Pirenzepine (M1 receptors), [^{3}H]AF-DX-384 (M2 receptors), and [^{3}H]cytisine (heteromeric nicotinic AChR) binding at the level of striatum of control (C) and transgenic (T) mice. The drawing is of level 15 (Swanson, 1992). **B:** [^{3}H]Pirenzepine (M1 receptors), [^{3}H]AF-DX-384 (M2 receptors), and [^{3}H]cytisine (heteromeric nicotinic AChR) binding and in situ hybridization of nicotinic AChR α7 mRNA at the level of the mesencephalon of C mice and T mice. The drawing is of level 39 (Swanson, 1992).

even reverse) this mild to moderate nonpathological cognitive decline.

Normal levels of AChR mRNAs and proteins

The expression levels and properties of AChR subtypes and several other synaptic proteins were normal in AChE-transgenic mice, as revealed by in situ hybridization, RT-PCR, and ligand binding experiments. Also, up to the age of 12 months there was no sign of cell death in their brains. The functional deficits that we observed previously in the capacity of these transgenic mice to respond to muscarinic and nicotinic drugs (Beeri et al., 1995; Andres et al., 1996) suggest that some modifications in receptor functioning in vivo did take place. In view of the similar expression and binding patterns of AChRs, the receptor loss in AD can tentatively be related to the reduced dendritic branching and spine formation rather than to production deficiences. This explains the relative resistance of AChE-transgenic mice as compared with control animals to the hypothermic effects of muscarinic and nicotinic agonists (Beeri et al., 1995; Andres et al., 1996), yet raises doubts as to the value of such agonists for treating AD patients with behavioral cholinergic deficits.

Regional enhancement in [^{3}H]hemicholinium-3 binding

Although ChAT mRNA levels remained unchanged in the transgenic brain, the rate-limiting step in ACh synthesis is choline reuptake into neuronal terminals (Wurtman, 1992). Forloni and Angeretti (1992) showed a >50% decrease in number of hemicholinium-3 binding sites in the striatum of aged rats. Using tissue from rapid autopsy, Slotkin et al. (1994) showed that choline uptake and [^{3}H]hemicholinium-3 binding are elevated in cortical regions but not the putamen of Alzheimer's patients, indicating that the rise in binding was specifically associated with regions undergoing cholinergic degeneration. The increase in hemicholinium-3 binding to the striatum of AChE-transgenic mice compared with controls suggests elevated choline uptake and ACh synthesis, as a compensatory reaction to ACh deficits. The twofold enhancement in hemi-

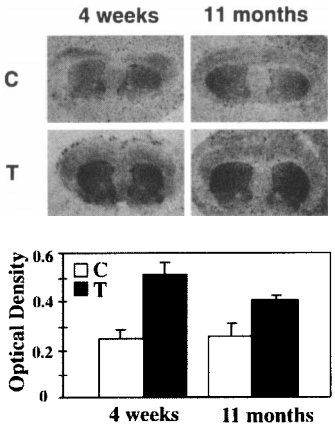

FIG. 6. Enhanced [^{3}H]hemicholinium-3 binding in transgenic neostriata. **A:** Autoradiography followed by image analysis. Binding was increased of [^{3}H]hemicholinium-3 to the neostriatum of 4-week- (**left**) and 12-month-old (**right**) normal mice (**top**; C) as compared with transgenics (**bottom**; T). Presented are brain sections following 2 weeks of exposure, indicating increased choline transport in these brain regions. **B:** Quantification of [^{3}H]-hemicholinium binding. Presented is one typical autoradiography experiment of four (n = 2 animals). For each animal, the images of two to six sections were digitized [at the neostriatum level, between level 21 and 30 of Franklin and Paxinos (1997)], and the MGV of the two hemistriata was recorded. See Materials and Methods for calculations. Data are expressed as mean ± SEM (bars) OD values.

cholinium binding was seen both in 4–5-week-old transgenic mice and in 11–12-month-old ones and could have contributed to imbalanced membrane metabolism, which may perhaps explain the attenuation in dendrite branching.

In conclusion, attenuated dendritic branching, reduced spine formation, impaired working and reference memory, and enhanced choline transport emerged in our work as primary neuroanatomical, behavioral, and metabolic correlates of pathological conditions that involve AChE overexpression and/or cholinergic imbalance. Therefore, AChE-transgenic mice should be most useful for exploring the mechanisms leading to these correlates. Moreover, the observed mechanisms for potential structural and metabolic compensation can shed new light on the late-onset, progressive nature of diseases associated with cholinergic imbalance. The observed progressive cognitive and motor deterioration in transgenic mice expressing human AChE in CNS (Beeri et al., 1995; Andres et al., 1996, 1997) could hence indicate the failure of control mechanism(s) to maintain this balance beyond a certain age.

Acknowledgment: This work was supported by USARMRDC grant 17-97-1-7007 and by Ester/Medica Neurosciences (to H.S.). R.B. was the recipient of an EMBO and an ENN short-term fellowships for the work in J.P.C.'s laboratory.

REFERENCES

Andres C., Beeri R., Huberman T., Shani M., and Soreq H. (1996) Cholinergic drug resistance and impaired spatial learning in transgenic mice overexpressing human brain acetylcholinesterase. *Prog. Brain Res.* **109,** 265–272.

Andres C., Beeri R., Friedman A., Lev-Lehman E., Henis S., Timberg R., Shani M., and Soreq H. (1997) ACHE transgenic mice display embryonic modulations in spinal cord CHAT and neurexin Iβ gene expression followed by late-onset neuromotor deterioration. *Proc. Natl. Acad. Sci. USA* **94,** 8173–8178.

Arendt T., Marcova L., Bigl V., and Bruckner M. K. (1995) Dendritic reorganisation in the basal forebrain under degenerative conditions and its defects in Alzheimer's disease. I. Dendritic organisation of the normal human basal forebrain. *J. Comp. Neurol.* **151,** 169–188.

Bartus R. T. and Uemura Y. (1979) Physostigmine and recent memory: effects in young and aged non-human primates. *Science* **206,** 1037–1089.

Beeri R., Andres C., Lev-Lehman E., Timberg R., Huberman T., Shani M., and Soreq H. (1995) Transgenic expression of human acetylcholinesterase induces progressive cognitive deterioration in mice. *Curr. Biol.* **5,** 1063–1071.

Bierer L. M., Haroutunian V., Gabriel S., Knott P. J., Carlin L. S., Purohit D. P., Perl D. P., Schmeidler J., Kanof P., and Davis K. L. (1995) Neurochemical correlates of dementia severity in Alzheimer's disease: relative importance of the cholinergic deficits. *J. Neurochem.* **64,** 749–760.

Braak H. and Braak E. (1985) Golgi preparations as a tool in neuropathology with particular reference to investigations of the human telencephalic cortex. *Prog. Neurobiol.* **25,** 366–368.

Buell S. J. and Coleman P. D. (1981) Quantitative evidence for selective dendritic growth in normal human aging but not in senile dementia. *Brain Res.* **214,** 23–41.

Coleman P. D. and Flood D. G. (1987) Neuron numbers and dendritic extent in normal aging and Alzheimer's disease. *Neurobiol. Aging* **8,** 521–545.

Coyle J. T., Price D. L., and DeLong M. R. (1983) Alzheimer's disease: a disorder of cortical cholinergic disruption. *Science* **219,** 1186–1189.

Davies P. and Maloney A. J. F. (1976) Selective loss of central cholinergic neurons in Alzheimer's disease. *Lancet* **2,** 1403.

DeKosky S. T. and Scheff S. W. (1990) Synapse loss in frontal cortex biopsies in Alzheimer's disease: correlation with cognitive severity. *Ann. Neurol.* **27,** 457–464.

Ferrer I. N., Guionnet F. C., and Tunon T. (1990) Neuronal alterations in patients with dementia: a Golgi study on biopsy samples. *Neurosci. Lett.* **144,** 11–16.

Fibiger H. C. (1991) Cholinergic mechanisms in learning, memory, and dementia: a review of recent evidence. *Trends Neurosci.* **14,** 220–223.

Fischer W., Gage F. H., and Bjorklund A. (1989) Degenerative changes in forebrain cholinergic nuclei correlate with cognitive impairments in aged rats. *Eur. J. Neurosci.* **1,** 34–45.

Forloni G. and Angeretti N. (1992) Decreased [^{3}H]hemicholinium binding to high-affinity choline uptake sites in aged rat brain. *Brain Res.* **570,** 354–357.

Franklin K. B. J. and Paxinos G. (1997) *The Mouse Brain in Stereotaxic Coordinates.* Academic Press, San Diego.

Gallagher M. and Colombo P. J. (1995) Aging: the cholinergic hypothesis of cognitive decline. *Curr. Opin. Neurobiol.* **5,** 161–168.

Games D., Adams D., Alessandrini R., Barbour R., Berthelette P., Blackwell C., Carr T., Clemens J., Donaldson T., and Gillespie F. (1995) Alzheimer-type neuropathology in transgenic mice overexpressing V717F β-amyloid precursor protein. *Nature* **373,** 523–527.

Gordon I., Grauer E., Genis I., Sehayek E., and Michaelson D. M. (1995) Memory deficits and cholinergic impairments in apolipoprotein E-deficient mice. *Neurosci. Lett.* **199,** 1–4.

Grauer E. and Kapon Y. (1993) Wistar–Kyoto rats in the Morris

water maze: impaired working memory and hyper-reactivity to stress. *Behav. Brain Res.* **59,** 147–151.

Hammond P., Rao R., Koenigsberger C., and Brimijoin S. (1994) Regional variation in expression of acetylcholinesterase mRNA in adult rat brain analyzed by in situ hybridization. *Proc. Natl. Acad. Sci. USA* **91,** 10933–10937.

Heidmann T. and Changeux J. P. (1978) Structural and functional properties of the acetylcholine receptor protein in its purified and membrane bound states. *Annu. Rev. Biochem.* **47,** 317–357.

Hodges H. (1966) Maze procedures: the radial-arm and the water maze compared. *Cognitive Brain Res.* **3,** 167–181.

Honer W. G., Dickson D. W., Gleeson J., and Davies P. (1992) Regional synaptic pathology in Alzheimer's disease. *Neurobiol. Aging* **13,** 375–382.

Hsiao K. K., Borchelt D. R., Olson J., Johannsdottir R., Kitt C., Yunis W., Xu S., Eckman C., Younkin S., Price D., Iadecola C., Clark B., and Carlson G. (1995) Age related CNS disorder and early death in transgenic FVB/N mice overexpressing Alzheimer amyloid precursor proteins. *Neuron* **15,** 1202–1218.

Hsiao K., Chapman P., Nilsen S., Eckman C., Harigaya Y., Younkin S., Yang F., and Cole G. (1996) Correlative memory deficits, Aβ elevation and amyloid plaques in transgenic mice. *Science* **274,** 99–102.

Katzman R. (1986) Alzheimer's disease. *N. Engl. J. Med.* **314,** 964–973.

LaFerla F. M., Tinkle B. T., Bieberich C. J., Haudenschild C. C., and Jay G. (1995) The Alzheimer's Aβ peptide induces neurodegeneration and apoptotic cell death in transgenic mice. *Nature Genet.* **9,** 21–30.

Le Novère N. and Changeux J. P. (1995) Ligand Gated Ion Channel Subunit Database. http://www.pasteur.fr/units/neubiomol/LGIC.html.

Le Novère N., Zoli M., and Changeux J. P. (1996) Neuronal nicotinic receptor α6 subunit mRNA is selectively concentrated in catecholaminergic nuclei of the rat brain. *Eur. J. Neurosci.* **8,** 2428–2439.

Leube R. E., Kaiser P., Seiter A., Zimbelmann R., Franke W. W., Rehm H., Knaus P., Prior P., Betz H., Reinke H., Beyreuther K., and Wiedenmann B. (1987) Synaptophysin: molecular organization and mRNA expression as determined from cloned cDNA. *EMBO J.* **6,** 3261–3268.

Mabry T. R., McCarty R., Gold P. E., and Foster T. C. (1996) Age and stress history effects on spatial performance in the swim task in Fischer-344 rats. *Neurobiol. Learn. Mem.* **66,** 1–10.

McEntee W. J. and Crook T. H. (1992) Cholinergic function in the aged brain: implications for treatment of memory impairments associated with ageing. *Behav. Pharmacol.* **3,** 327–336.

Moran P. M., Higgins L. S., Cordell B., and Moser P. C. (1995) Age related learning deficits in transgenic mice expressing the 751-amino acid isoform of human β-amyloid precursor protein. *Proc. Natl. Acad. Sci. USA* **92,** 5341–5345.

Morris R. (1984) Development of a water-maze procedure for studying spatial learning in the rat. *J. Neurosci. Methods* **11,** 47–60.

Nordberg A., Adem A., Hardy J., and Winblad B. (1988) Change in nicotinic receptor subtypes in temporal cortex of Alzheimer brain. *Neurosci. Lett.* **86,** 317–321.

Perry E., Morris C., Court J., Cheng A., Fairbairn A., McKeith I., Ieving D., Brown A., and Perry R. (1995) Alteration in nicotine binding sites in Parkinson's disease, Lewy body dementia and Alzheimer's disease: possible index of early neuropathology. *Neuroscience* **64,** 385–395.

Picciotto M. R., Zoli M., Lena C., Bessis A., Lallemand Y., Le Novère N., Vincent P., Pich E. M., Brulet P., and Changeux J. P. (1995) Abnormal avoidance learning in mice lacking functional high-affinity nicotine receptor in the brain. *Nature* **374,** 65–67.

Price D. L., Sisodia S. S., and Gandy S. E. (1995) Amyloid β amyloidosis in Alzheimer's disease. *Curr. Opin. Neurobiol.* **8,** 268–274.

Purpura D. P. (1974) Dendritic spine "dysgenesis" and mental retardation. *Science* **186,** 1126–1128.

Seidman S., Sternfeld M., Ben Aziz-Aloya R., Timberg R., Kaufer-Nachum D., and Soreq H. (1995) Synaptic and epidermal accumulations of human acetylcholinesterase are encoded by alternative 3′-terminal exons. *Mol. Cell. Biol.* **15,** 2993–3002.

Sholl D. A. (1953) Dendritic organization in the neurons of the visual and motor cortices of the cat. *J. Anat.* **87,** 387–406.

Slotkin T. A., Nemeroff C. B., Bissette G., and Seidler F. G. (1994) Overexpression of the high affinity choline transporter in cortical regions affected by Alzheimer's disease. *J. Clin. Invest.* **94,** 696–702.

Swanson L. W. (1992) *Brain Maps: Structure of the Rat Brain.* Elsevier, Amsterdam.

Terry R. D., Masliah E., Salmon D. P., Butters N., De Teresa R., Hill R., Hansen L. A., and Katzman R. (1992) Physical basis of cognitive alterations in Alzheimer's disease: synapse loss is the major correlate of cognitive impairment. *Ann. Neurol.* **30,** 572–580.

Valverde F. (1976) Aspects of cortical organization related to the geometry of neurons with intra-cortical axons. *J. Neurocytol.* **5,** 509–529.

Vickroy T., Roeske W., and Yamamura H. (1984) Sodium-dependent high-affinity binding of [^{3}H]hemicholinium-3 in the rat brain: a potentially selective marker for presynaptic cholinergic sites. *Life Sci.* **35,** 2335–2343.

Wellman C. L. and Sengelaub D. R. (1995) Alterations in dendritic morphology of frontal cortical neurons after basal forebrain lesions in adult and aged rats. *Brain Res.* **669,** 48–58.

Whitehouse P., Martino A., Antuono P., Lowenstein P., Coyle J., Price D., and Kellar K. (1986) Nicotinic acetylcholine binding sites in Alzheimer's disease. *Brain Res.* **371,** 146–151.

Wurtman R. J. (1992) Choline metabolism as a basis for the selective vulnerability of cholinergic neurons. *Trends Neurosci.* **15,** 117–122.

Zhi Q. X., Yi F. H., and Xi C. T. (1995) Huperzine A ameliorates the spatial working memory impairments induced by AF64A. *Neuroreport* **6,** 2221–2224.